THE ASTRONOMICAL JOURNAL VOLUME 98, NUMBER 6 DECEMBER 1989

THE BINARY-RICH CLUSTER ABELL 2244

JAMES M. SCHOMBERT AND MICHAEL J. WEST
Department of Astronomy, University of Michigan, Ann Arbor, Michigan 48109

JOSHUA R. ZUCKER
Department of Astronomy, California Institute of Technology, Pasadena, California 91125

MITCHELL F. STRUBLE
Department of Astronomy and Astrophysics, University of Pennsylvania, Philadelphia, Pennsylvania 19104-6394
Received 21 March 1989; revised 14 August 1989

ABSTRACT

A structural, luminosity, and velocity study of the cluster Abell 2244 is presented. A2244 was selected for study from the list of Struble and Rood because of its unusually binary-rich population in an evolved cD-type cluster environment, a contradiction in terms of cluster collapse scenarios versus the formation and survival of bound pairs. In comparison with the Coma cluster, A2244 is a slightly poorer version with a suspected deficiency in the number of cluster members in the core. This evidence, combined with the high-velocity dispersion of the cluster, suggests that a low-velocity population of galaxies has been consumed by the central cD galaxy. The central cD galaxy has a single low-velocity companion deep in its envelope and cross sections of its surface-brightness profile suggest that it is in transition from a depressed central surface-brightness object to a high central concentration system, a point of contention in merger models. All but two of the binary galaxies were found to be projections with other cluster members or stars and, thus, are not in conflict with the advanced dynamical age of the cluster.

I. INTRODUCTION

The details of postcluster collapse evolution are not, observationally, well known. Theoretical work, both analytic and N body, has predicted a wide range of phenomenon (mass segregation, tidal stripping, cannibalism, gravitational focusing, etc.) which, for the most part, have remained elusive to quantitative generalization. As usual with many lines of astronomical research, one approach to better understanding is to study objects with peculiar characteristics on the asumption that they are perturbed and, therefore, reflect some underlying process that can be identified.

A study of a cluster of galaxies, peculiar in the sense of being rich in binaries, is of particular interest for two reasons. The first is that velocity information on a large enough sample of binaries can provide clues to the local $\mathscr{M}/L$'s of the galaxy pairs while simultaneously providing a global value of the cluster velocity dispersion and $\mathscr{M}/L$. In contrast, most of our knowledge of the masses of galaxies is quantized on scales from rotation curves (0–50 kpc), to field binaries (10–70 kpc) and cluster velocity dispersions (100 kpc to 4 Mpc), which is not a collection uniform in environment or galaxy type. Of secondary interest is the fact that most theories of cluster evolution suggest binaries should be disrupted during initial collapse and violent relaxation. The dynamics of binary galaxies have long been of interest to extragalactic astronomy, particularly since their study yields information about galaxy total masses and $\mathscr{M}/L$'s (Schweizer 1987; White *et al.* 1983). However, binary galaxies studied to date have been primarily nearby field systems. The existence of bound binaries in a cluster of galaxies was thought to be rare, or restricted to first-ranked members, due to the strong tidal effects and high collisional probabilities experienced by galaxies in dense environments. For example, work by Heggie (1975) showed that "soft" binary stars in clusters (those with $\Delta v < \sigma$) are easily disrupted and, since the velocity dispersion of clusters of galaxies are much higher than the typical Δv's of field binaries, their numbers should be small. This is due primarily to the numerous encounters in the early stages of cluster collapse and would quickly dissolve any cluster binaries.

From the above scenarios, there is the expectation that a binary-rich cluster is either a dynamically young system or is produced by some process that has preserved the number of binaries after collapse. Thus, the discovery by Struble and Rood (1981) of a cD cluster (a cluster assumed to be well evolved dynamically) from a list of ten Abell clusters that are abundant in the number of binary galaxies among normal cluster members is surprising and, at the very least, without theoretical basis. The purpose of this paper is to use velocity and photometric data on normal and binary galaxies in this cluster as a probe into the formation and evolution of clusters and their galaxy population. And, as seen below, to show how this cluster serves as an example of a system in an advanced state of dynamical evolution.

II. OBSERVATIONS

a) Object Selection

The cluster and the sample of binary galaxies was selected from the list of Struble and Rood (1981). A majority of these clusters were Rood/Sastry types I and F, which is usually interpreted as an indicator of a dynamically young cluster morphology. A2244 was selected for the present study since it is the only cD cluster in the binary-rich list, which is peculiar since cD clusters are assumed to be dynamically evolved and, thus, unlikely to possess many binary pairs as three-body interactions would presumably disrupt any bound configurations. As a class, cD clusters have the smallest fraction of binaries, among their brightest members, of all the RS types (Struble and Rood 1987a) consistent with the above hypothesis.

Object selection began with inspection and positional

 0004-6256/89/061999-19$00.90

measurements from IIIa-J plates of the Second Palomar Sky Survey. During this inspection a visual classification of star versus galaxy identity was made. The smaller grain size in the emulsion for the Second Sky Survey made eye classification trivial to an apparent magnitude of 19. This was of great importance since such inspection showed immediately that several of the binaries were simply galaxy–star pairs or multiple galaxy systems (see Sec. IIIc). A measure of success in the star/galaxy classification is taken from the fact that none of the objects identified as galaxies and selected for later spectroscopic observations were indeed at redshifts greater than 2000 km s^{-1}.

CCD frames were obtained for most of the binaries identified above in order to determine luminosities. As well as individuals, a CCD frame mosaic was made of the inner 0.25 Mpc of the cluster. This mosaic was used for the construction of the luminosity function and the calculation of cluster density (see Sec. III*a*). For conversion to kpc and absolute magnitude, a $H_0 = 100$ km s^{-1} Mpc^{-1} and a $q_0 = 0$ have been assumed throughout this paper.

b) Photometry

Photometry for this study was based on a mosaic of CCD frames taken with the Palomar 1.5 m telescope. The detector was a TI 800×800 CCD array with a readout noise of nine electrons. The photometry was calibrated using standards taken from the list of Landolt (1985). Exposure times were 600 s for *B* frames and 300 s for *V* frames. Each frame was bias subtracted after each exposure from averages of 50 overscan lines and rebinned to 400×400 for a final scale of 0.47 arcsec per pixel. The frames were flattened from dome flats taken at various times during the night near the airmass of the observations. All the nights were photometric with an average seeing of 1.5 arcsec.

The final stages in photometry reduction were performed with the software package ARCHANGEL, an overseer program to the GASP reduction system (Cawson 1983). The first step in this process is the determination of the sky level and its variation on the scale of the observed region. An average of 8–10 sky boxes of 20×20 pixels were selected interactively on regions of the frame devoid of stars and distant from the primary object. Deviations from the mean of these boxes indicates that the *B* frames were flat to 0.3% level and *V* frames were flat to the 0.5% level. Each frame was then cleaned of cosmic rays and stars near the object of interest, which could distort the contour-fitting routines.

The next phase of the reduction consisted of aperture photometry. The method used here deviates from normal aperture work by electing to use elliptical apertures rather than circular ones. This is done for two reasons. The first is that the use of an ellipse provides a much closer match to the outer contour of a galaxy than a circle, thus minimizing the sky noise. Second, parameters of this ellipse, calculated from the moment analysis above a set threshold, can be tabulated to provide some sense of the outer structure and shape of each galaxy. All the photometry was isophotal with the 25 V mag $arcsec^{-2}$ level selected as the threshold. Contact binaries were analyzed with their companions masked out and masked regions interpolated. Typical errors were ± 0.02 mag.

c) Spectroscopy

Galaxies in the field of the cluster A2244 were observed on the nights of 25–28 May and 4 and 5 August 1988 at the Hale 5 m telescope using the double spectrograph (DBSP, see Oke and Gunn 1982). The detectors were two TI 800×800 CCDs. The blue side CCD was enhanced with an oxygen purging technique to bring its quantum efficiency to 40% at 4000 Å. On the blue side, a 300 lines/mm 3990 Å first-order grating was used, which covered the wavelength range 3850–5500 Å at 2.1 Å per pixel. The red side was adjusted to cover from 500 to 7900 Å using a 316 lines/mm 7150 Å first-order grating resulting in 3.0 Å per pixel. The slit used was 2 arcsec wide and 2 arcmin long rotated to various position angles so as to cover both galaxies in each binary. Exposure times ranged from 600 to 1200 s depending on the brightness of the galaxies. Guiding was performed with a Quantex image system directly off the back-silvered slit, usually on an off-center star or the galaxies themselves. Flatfields were taken in the middle of the cluster program and comparison lamps were taken either before or after each exposure (Fe-Ar in the blue, Ne-Ar-He in the red). The weather conditions for the run were clear with 1–2 arcsec seeing.

Reduction was performed using a modified version of the software package FIGARO developed by K. Shortridge (AAO). Initial reduction at the telescope consisted of subtracting an erase level determined by overscans, and then dividing each spectrum by a flatfield. After flatfielding the images, regions of sky and object were determined. Then, a cubic polynomial was fit along each wavelength bin of the sky regions, rejecting any deviant pixels in order to avoid bad pixel rows and cosmic rays. This sky fit was then subtracted from the image.

The galaxy spectrum was then extracted using an optimal extraction algorithm. For each pixel in the spatial direction, this algorithm fits a 7th order polynomial along the dispersion. Deviant pixels, such as spectral lines and cosmic rays, are rejected in the initial fit. Then, moving along the dispersion, the spatial profile of the object is compared to the spatial profile of the polynomials. A cosmic ray will distort the spatial profile of the image, and thus can be rejected, while spectral lines share the spatial profile and are preserved. The extraction is then weighted by the predicted signal-to-noise ratio, with noise approximated as a constant value (the readout noise of the CCD), plus a term proportional to the square root of the counts. Ideally, this noise approximation would include predicted sky values, but in this implementation only the sky-subtracted image was used. Finally, the weights for each pixel are normalized to conserve the flux at each wavelength. This weighting procedure also corrects for minor S distortion, since a 7th order polynomial can react to some curving of the spectrum. The arc spectrum that corresponds to the galaxy was extracted using the same pixel weights to ensure proper correspondence.

After one arc had been fit by a fourth-order polynomial, and as many lines identified as possible, the rest of the arcs were fit by cross correlating the arc spectra and then shifting the polynomial to maximize the correlation. As the rms error of these shifted fits was essentially the same as in the original fit (i.e., 0.6 Å), use of the same polynomial for all the arcs should give a more consistent wavelength fit, and thus lead to more accuracy in the final calculations. The wavelength calibration on the arc spectrum was then copied to the spectrum of the object corresponding to that arc.

After extraction, the data were scrunched into 800 linear bins for each camera. The scrunched data were then interpolated across the dichroic break at 5500 Å. The raw data were then extinction corrected using the standard Palomar tables.

Flux calibration was performed using Fiege 110 and BD +28° 4211 as primary standards (Massey *et al.* 1988). The difference in calibration between the beginning and end of night standards was always less than 3% and, thus, an average calibration curve was used for each camera. The spectrum of the central cD galaxy is shown in Fig. 1. The primary features for the cross-correlation algorithm are Ca II *H*, *K*, and G bands on the blue side and Mg *B* and Na I *D* on the red side. The noise at 5500 Å is where calibration across dichroic breaks down.

The flux-calibrated spectra were then examined for the location of the Hα emission lines from which the velocities were to be calculated. A region surrounding those lines was selected, including as much data as possible without introducing atmospheric absorption bands. Then, a quadratic polynomial was fit to the underlying continuum to obtain an initial estimate of its level, after which a Gaussian profile was added for each spectral line to be fit. To ensure that there would be no confusion in the Hα/N II blend, the ratio of the centers of the three lines were fixed, along with the ratio of the amplitudes of the two nitrogen lines. Similarly, for the S II doublet, the ratio of the centers was fixed, and the centers with respect to Hα also fixed. The "best" fit, using χ^2 as a measure, was then found using a slight modification of the Marquardt minimization algorithm. Note that as a constant σ model was used, the χ^2 minimization was in reality a least-squared-error approach. The integrated intensities, FWHM, and so forth were then calculated using the analytic functions since overlap would distort any attempt to use the raw data. This procedure was applied on a column-by-column basis to the only object with Hα emission, binary 16 (see Sec. III*d*), in order to produce a rotation curve. The true power of this technique is the ability to constrain the centers of the lines within the fit, reducing the formal error to ± 20 km s^{-1}.

Objects with only absorption features were cross correlated using an algorithm similar to that of Tonry and Davis (1979). Rather than cross correlating with a template star, it was elected to make comparison with the galaxy NGC 6166 in A2199. This has the advantage of cross-correlating objects with the same basic spectral energy distribution and absorption-line features. Several exposures of NGC 6166 were taken during the run and the difference in velocities was always less than 15 km s^{-1}. To convert the relative velocities to a standard heliocentric frame, we have assumed a velocity of 9348 km s^{-1} for NGC 6166 (Tonry 1985). There was some difficulty in the procedure since the Mg *B* feature passes from the blue to the red side of the spectrograph as one goes from A2199 to A2244. An additional check was performed by cross correlating the individual cluster members with the central cD galaxy. Each side of the spectrograph was cross correlated independently, then weight averaged. A check on the internal errors is provided through comparison between the velocity measurement as determined from the blue side with the result from the red-side spectra. Since both sides of the DBSP operate separately, the two measurements are independent below the point where the dichroic splits the incoming light. The mean from the difference between the blue

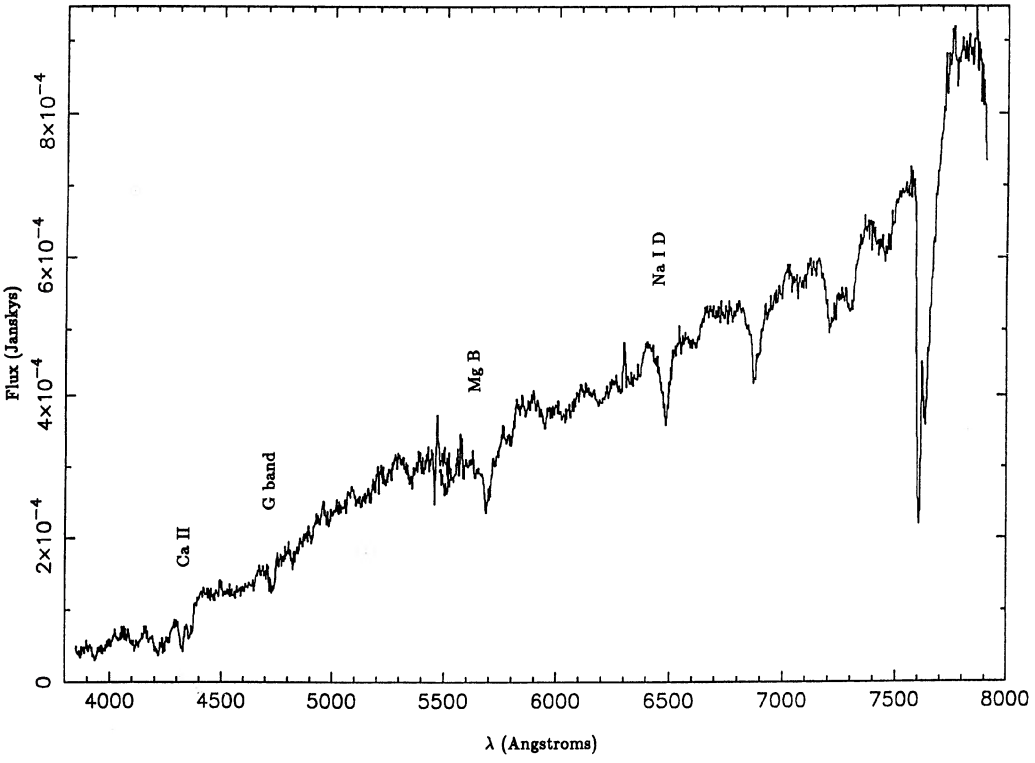

FIG. 1. Sample spectrum of the cD galaxy in A2244. Features of interest for the cross-correlation technique are the Ca II *H* and *K* lines and the G band on the blue side, Mg *B* and Na I *D* lines on the red side. The excess noise at 5500 Å is the junction from the dichroic for the blue and red sides of the double spectrograph. Features to 6600 Å are atmospheric bands.

and red sides is 18 km s^{-1} with a dispersion of 75 km s^{-1}. A typical error based on the comparison to external error of 60 km s^{-1} was adopted. Table I lists the cD, its companion and the nonbinary members of the cluster. Table II presents the data for the binary pairs. Each pair is identified as east or west, where the E or W designation simply means the most eastern or most western of the pair regardless of position angle. Column 1 of both tables displays an identification number of the object (arbitrarily assigned). Columns 2 and 3 present the X and Y coordinates in arcsec from the center of the cD galaxy. Column 4 presents the distance from the cD galaxy in kpc. Column 5 presents the velocity with respect to the cD galaxy or indicates if the object was a star. For conversion to heliocentric velocities, a velocity of 28 625 km s^{-1} was adopted from the average of multiple exposures of the cD galaxy.

III. DISCUSSION

a) Cluster Properties

Morphologically, A2244 is classified as a cD-type cluster on the Rood and Sastry (RS) scheme (Struble and Rood 1987a). However, its Bautz–Morgan (BM) type (Leir and van den Bergh 1977) is class II implying that, although the core of A2244 is dominated by an extended, centrally located cD galaxy, this dominance is not as extensive as a classic cD cluster such as A1413 or A2670. There are several other bright galaxies in the cluster, but the cD galaxy is the first-ranked member. The richness of A2244 in Abell counts is 89 (Abell 1958). On the assumption that the morphological classifiers are some coarse indicator of the dynamical state of a cluster, then A2244 would seem to be advanced in its evolution, at least in a post-collapse phase as compared to *N*-body simulations (White 1979; West *et al.* 1987). The cD galaxy in A2244 has an absolute magnitude of -22.0 and a diameter of 98 kpc at the 25 V mag $arcsec^{-2}$ isophote.

The well-studied Coma cluster (A1656) is in many ways similar to A2244 and a comparison between the two is informative. Coma has a RS class of *B*, a BM class of II, and a richness of 109 (see Table IV). The Coma cluster, despite its *B* or binary RS class, also has a cD galaxy at its core (NGC 4874, Schombert 1988). The Coma cluster is classified as a *B* type because of the existence of two giant ellipticals, NGC 4874 and NGC 4889, within the cluster core. Aperture magnitude places NGC 4889 as the brighter member, but this fails to account for the light of the extended envelope around NGC 4874. Also, Coma has two apparent subgroups, the more dominant in the galaxy and velocity distribution are

TABLE I. A2244 cluster members.

Object	X (arcsec)	Y (arcsec)	R (kpc)	Δv (km s^{-1})
1	...	...	...	...
1N				−68
2	37E	4S	46	−1604
3	84W	89N	150	62
4	95W	106N	175	−102
5	137W	131S	233	−1014
6	125W	160S	250	−1157
7	28W	49S	69	1795
8	44W	21S	60	−1171
9	74W	48S	108	937
10	106W	51S	145	1612

TABLE II. A2244 binaries.

Object	X (arcsec)	Y (arcsec)	R (kpc)	Δv (km s^{-1})
B1E	70W	16S	88	...
B1W				...
B2E	148W	87S	211	-927
B2W				939
B3E	89E	137S	201	-1256
B3W				-913
B4E	9E	266S	327	-604
B4W				star
B5E	37E	61N	88	1053
B5W				star
B6E	253W	84N	328	2315
B6W				-233
B7E	208W	113N	291	488
B7W				-555
B8E	105E	197N	275	...
B8W				star
B9E	92W	315S	404	19,170
B9W				2470
B10E	388W	370N	659	...
B10W				...
B11E	86E	284N	365	67,190
B11W				1281
B12E	85E	508N	634	star
B12W				...
B13E	400E	615N	902	...
B13W				star
B14E	367E	385N	654	...
B14W				...
B15E	46W	779E	960	...
B15W				star
B16E	138W	849S	1,058	2605
B16W				2805
B17E	500W	820S	1,181	...
B17W				star
B18E	123W	57N	167	-808
B18W				2132

centered on NGC 4874 (Fitchett and Webster 1987). The interpretation is that Coma is in a transition stage, with more cD-like than *B*-type cluster properties. The absolute magnitude of NGC 4874 is -22.0, identical to the cD galaxy in A2244. Therefore, A2244 and Coma are similar in cluster appearance and cD galaxy properties, with Coma being slightly richer than A2244.

The global richness from Abell counts of A2244 is 16% lower than Coma. To confirm this all galaxies were counted from a mosaic of *V* band CCD frames within 0.25 Mpc of the cD galaxy. These data were then compared to the Godwin and Peach (1977) survey of the Coma cluster. Both samples were trimmed to the Coma completeness limit of $M_V = -16.7$ (although the CCD data were deeper). The resulting distribution is shown in Fig. 2, where each galaxy is plotted as a circle whose size represents the 25 V mag arcsec^{-2} isophotal size (eccentricity data were not available from Godwin and Peach and, hence, is suppressed in the A2244 plot). The two largest galaxies in Coma are NGC 4874 on the right and NGC 4889 on the left. The cD galaxy in A2244 is the most prominent object in the center of the figure. Simply from examining the distribution plots in Fig. 2, it is obvious that A2244 is less rich than Coma. The actual value from galaxy counts is that A2244 contains 34% fewer galaxies in the inner 0.25 Mpc than Coma. The background/foreground corrections for both clusters are negligible because of the high luminosity cutoff used and the small angular size for A2244. There is also a visual impression that the number of objects near the cD galaxy NGC 4874 in Coma is much higher than the cD galaxy in A2244, even after correction for the higher richness of Coma as a whole. This is confirmed in a plot of galaxy density ratio between A2244 and Coma as a function of radius shown in Fig. 3. The projected galaxy density drops from a mean value of 63% at 200 kpc to 42% for the inner 50 kpc ring. The interpretation is that either A2244 is deficient in galaxies in the core or Coma is overabundant. Three possible explanations arise for this difference. One is that Coma has a cusp in its galaxy distribution of the type proposed by Beers and Tonry (1986); in which case the profile for A2244 is depressed and Coma is sharply peaked. However, all evolved clusters (including A2244) should be peaked in this scheme. The second explanation invokes dynamical friction on the core of Coma where NGC 4874 has enhanced the number of the galaxies in its surroundings (Struble 1979; Lecar 1975). However, a third and equally plausible scenario is that the distribution in Coma is normal, whereas the cD galaxy in A2244 has consumed its neighbors, thus producing a deficiency in its neighborhood. It is this last interpretation that will be supported with observations of the cD galaxy in Sec. III*c*.

The cluster luminosity of Coma, calculated for the inner 0.25 Mpc from the Godwin and Peach data is $1.4\times10^{12}\,L_\odot$. The same calculation for A2244 yields $3.9\times10^{11}\,L_\odot$, 28% of the value of Coma. This is 67% the value expected from the number counts and implies that A2244 is even more underluminous than Coma in its core. Dynamical evolution could account for this in two ways. One is to strip the core galaxies by the cluster mean field where, on average, each galaxy loses $\frac{1}{3}$ of its light to the general intracluster medium. Since the number counts are done in a magnitude complete fashion, yet the luminosities are determined by isophotal means, then a large, diffuse intracluster medium would not be measured [e.g., a large cD envelope, Schombert (1988)]. The second method is to cannibalize bright galaxies at a rate higher than faint galaxies. This removes light faster than actual objects per Mpc^3 and has support from models of dynamical friction, which predict faster evolution for high-mass objects. There is also support for this hypothesis in the weak evidence for luminosity segregation in both Coma and A2244. This was tested by dividing the samples into two

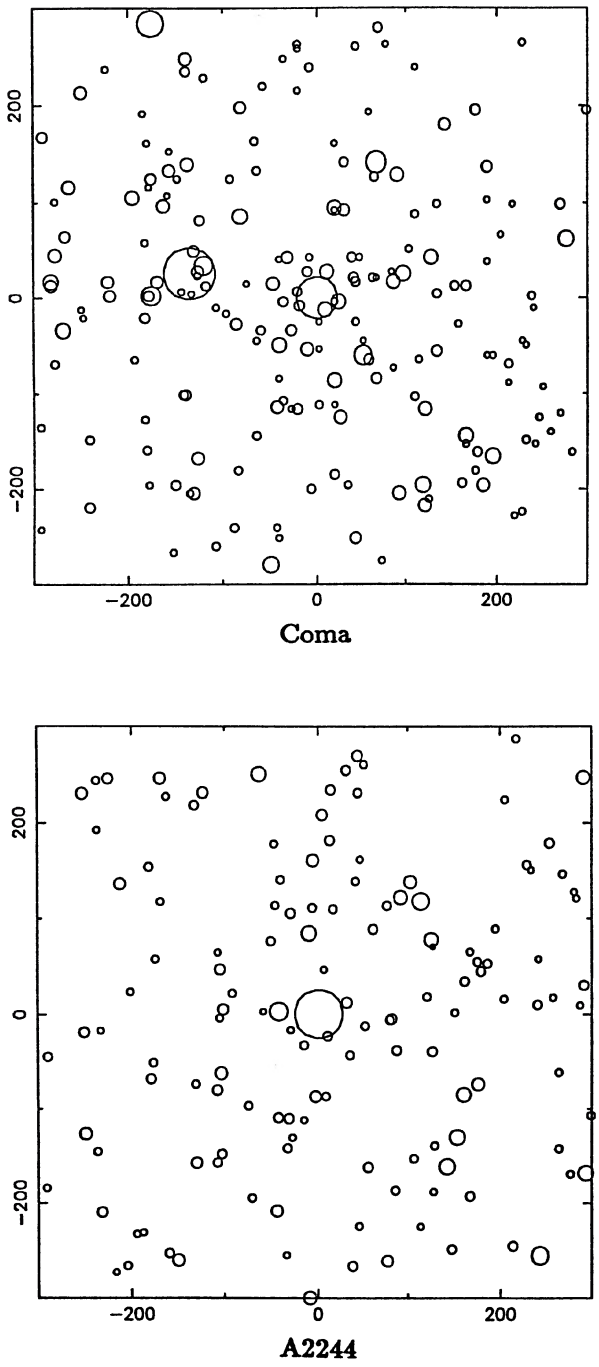

FIG. 2. Distribution of galaxies greater than $M_V = -16.7$ for Coma (top) and A2244 (bottom). Symbol sizes are scaled to match galaxy size (but not ellipticity) at the 25 V mag arcsec^{-2} isophote. Axes are in kpc with respect to the cD galaxy in each cluster.

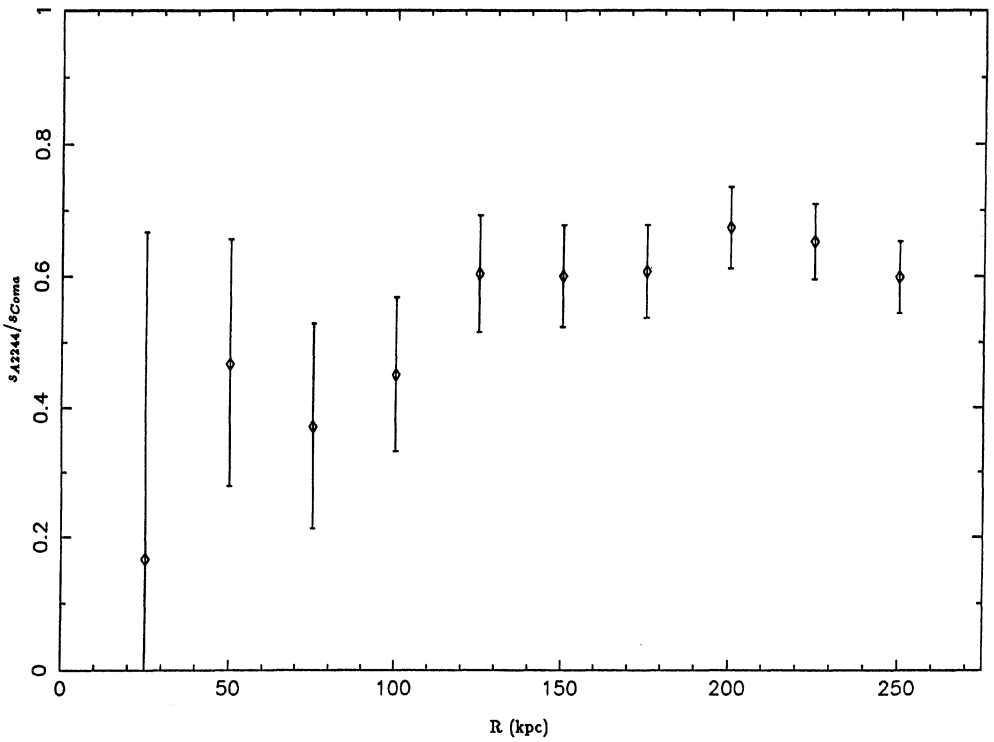

FIG. 3. Ratio of galaxy projected density for A2244 vs Coma as a function of radius. The projected density drops from 63% at 200 kpc to 42% in the core, indicating that A2244 is deficient in core objects with respect to Coma.

luminosity groups (one group with luminosities greater than $\frac{1}{2}L_*$, the other less than $\frac{1}{2}L_*$) and plotting the ratio of the two groups as a function of radius. This plot is seen in Fig. 4. There is a clear trend in that the ratio of faint to bright objects is decreasing from a mean value of 0.63 at 250 kpc to a core value of 0.45. However, this trend is only statistically significant at the 94% level based on a χ^2 test.

A summary of the dynamical information on A2244 is found in Table III. These values are determined from 27 redshifts (including unbound binaries) from Tables I and II. The velocity dispersions are calculated in the manner of Danese *et al.* (1980). The radial-velocity dispersion, ($\sigma_r = 1240$ km s^{-1}), is high but within the range of observed cluster values (Struble and Rood 1987b; Zabludoff, Huchra, and Geller 1989). The resulting core $\mathcal{M}/L$ is $\sim$1200 calculated in a fashion similar to Postman *et al.* (1989) where the harmonic radius was determined to be 0.4 Mpc (Coma value is 0.6 Mpc, see Hickson 1977), a visual to blue conversion of 1.5 was used and the cluster luminosity quoted above was increased by a factor of 2 to account for luminosity outside the core. We interpret the high $\mathcal{M}/L$ as further evidence of a deficiency of core members in A2244. The velocity of the cD galaxy is 350 km s^{-1} from the cluster mean, not an uncommon phenomenon for cD galaxies but usually associated with irregular cluster structure as well (Bothun and Schombert 1988). A summary of the luminosity and structural properties for A2244 plus a comparison with Coma values is found in Table IV. The galactic latitude listed in Table IV is relevant to the discussion of galaxy/star confusion of binaries in Sec. III*c*.

b) cD Galaxy

Although this paper is primarily concerned with binaries and their velocity distribution, the cD galaxy in the center of A2244 is also worthy of closer scrutiny. Morphologically, this object is similar to other cD galaxies from the samples of Oemler (1976) and Schombert (1988). It is not the brightest cD galaxy, but close to the mean in luminosity ($M_V = -22.0$) and radius ($r_{25} = 49$ kpc). The outer isophotes are of low eccentricity ($b/a = 0.9$) which is atypical for cD galaxies where Porter (1988) quotes a mean $b/a = 0.65 \pm 0.15$.

There is a clear anomaly in the core of the cD galaxy. This can be seen in Fig. 5, a low contrast close up of the inner 50 kpc. A first impression is that the central region or core is offset from the outer isophotes by approximately 3 arcsec (4 kpc). However, a more detailed examination of the contours reveals that the isophotes are clearly elliptical to the center and that the offset nucleus is, in fact, a companion object. This can be more clearly seen in Fig. 6, a cross cut from the center of the cD galaxy (as determined from the mean of the outer isophotes) through the companion. The companion lies about 2.5 arcsec south of the center. The cD galaxy has a peak surface brightness of 20.5 V mag arcsec^{-2}, whereas the companion has a peak surface brightness of 19.8.

The companion was also confirmed spectroscopically. The slit on the DBSP was turned to a position angle of 170° so as to integrate on the central cD body as well as the companion. The resulting velocity difference for the companion was 50 ± 50 km s^{-1}. Thus, unlike a majority of the compan-

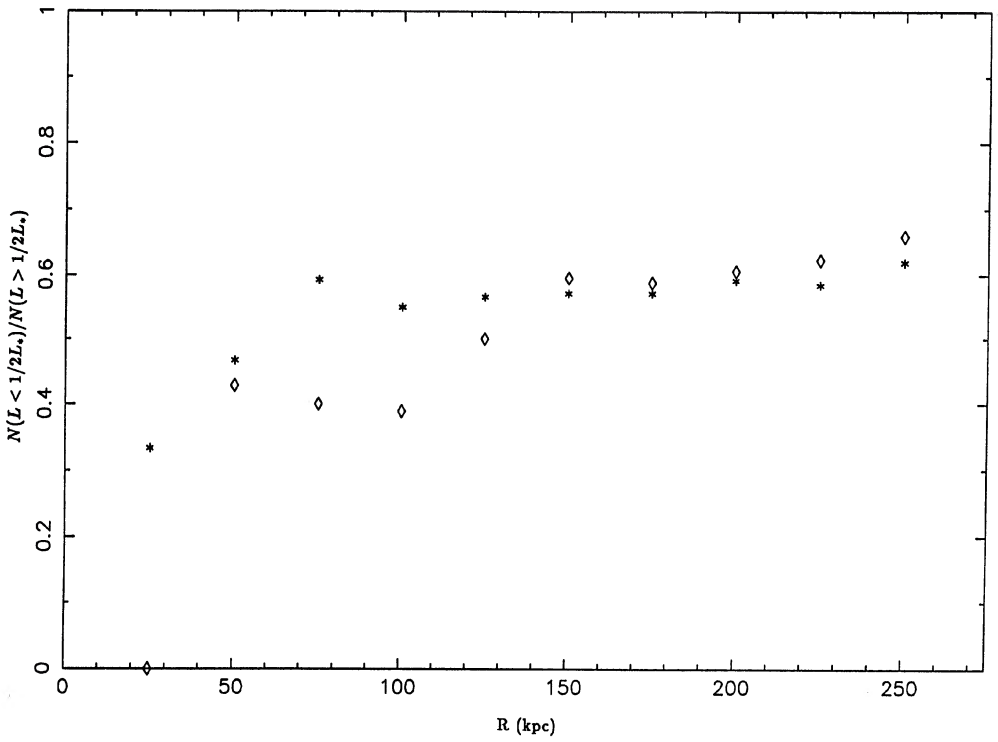

FIG. 4. Ratio of faint ($L<\frac{1}{2}L_*$) to bright galaxies ($L>\frac{1}{2}L_*$) for A2244 (◇) and Coma (*). There is weak evidence for luminosity (mass) segregation in both A2244 and Coma with A2244 being slightly deficient in bright core galaxies.

ions for cD galaxies that have radial velocities in excess of 800 km s^{-1} (Tonry 1985), this companion appears to be bound and nearing the final stages of cannibalism (i.e., its velocity approaches the mean of the cD galaxy).

An interesting point is the difference between the inner surface brightnesses of the cD galaxy and the companion. Most cD galaxies have high inner surface brightness from 18.0 to 19.5 V mag arcsec^{-2} and small core radii (Oemler 1976; Schombert 1986), similar to other bright ellipticals. However, there exists a distinct class of cD galaxies that have low central surface brightnesses and large core radii. A85 is a good example with a central surface brightness of 20.2 V mag arcsec^{-2} [see Fig. 2(e), Schombert 1987]. This separation into two classes, cD galaxies with normal inner surface brightnesses and cD galaxies with depressed inner surface brightnesses, is reminiscent of the differences between the Ostriker–Hausman models for cD growth (Ostriker and Hausman 1977, hereafter referred to as OH) and the N-body simulations of Duncan, Farouki, and Shapiro 1983, hereafter referred to as DFS). The OH models assumed an underlying principle of homology or conservation of energy and scale. The result was that, after each merger, the inner surface brightness decreases and the core radius increases. The DFS simulations indicate that homology assumptions are violated when postmerger relaxation restores the central concentration after a short phase with a depressed core. They also note that often the merging galaxy was only disrupted in the outer envelope and that the infalling galaxy's core could survive intact as dynamical friction reduced its motion to zero. This was also noted by White (1982) and it is these high-surface-brightness remnants that serve to increase the inner surface brightnesses of cD galaxies. Thus, the interpretation of the cD galaxy in A2244 is one where we are witnessing that final stage of merging, the transition from a OH-type low inner-surface-brightness body to a normal cD core with the capture of a high-surface-brightness companion. The final configuration will be similar in appearance to other bright cD galaxies (e.g., A1413), and the slow relative velocity of the companion suports the hypothesis that dynamical friction is almost completed.

An interesting thought experiment is to assume that the velocity dispersions of Coma and A2244 were once identical, but that the depletion of low-velocity objects in the core has artificially increased the measured velocity dispersion in

TABLE III. Dynamics summary.

Cluster	R.A. (1950) Dec	$<z>$	$<\sigma_r>$	$<\sigma_t>$	ΔV_{cD}
A2244	1700.9 + 3408	0.0968 ± 0.0008	1240^{+208}_{-138}	2115^{+407}_{-299}	350

TABLE IV. A2244/Coma comparison.

	A2244	Coma
$< z >$	0.097	0.023
N_{Abell}	89	106
RS type	cD	B/cD
M_{cD}	−22.0	−22.0
BM type	II	II
$N_{Binaries}$	18[a]	2
$\Sigma_{0.2\ Mpc}$	263 gal/Mpc^2	390 gal/Mpc^2
$\Sigma_{50\ kpc}$	446 gal/Mpc^2	955 gal/Mpc^2
σ_{cl}	1240 km/sec	880 km/sec
b_{II}	36°	88°

Note to TABLE IV

[a] Seven pairs were found to be star/galaxy pairs, see text.

A2244. Low-velocity or bound populations have been detected in several cD clusters (e.g., A2589, see Bothun and Schombert 1988) with typical properties of a mean Δv of 200 km sec^{-1} and a luminosity of $\frac{1}{2}$ L_* per member. A numerical simulation can be run to add this population back to the velocity distribution of A2244 in order to calculate the "missing" population's light as a function of velocity dispersion. An algorithm is used that generates a Gaussian distribution for the bound population of an input velocity dispersion from which n galaxies (where n is the variable of the experiment) are selected at random to be added to the velocity sample of A2244 and the velocity dispersion of the cluster as a whole then recalculated. This is run many times for each value of n and bound population dispersion to produce a mean change in the measured cluster dispersion as a function of n. The results are shown in Fig. 7, a plot of the number of objects and the recalculated cluster dispersion for the bound population dispersions of 1200, 500, 250, and 150 km s^{-1}. The run of 1200 km s^{-1} was performed to estimate the effect of simply increasing the sample size of normal cluster members. The fact that the new cluster dispersion decreases,

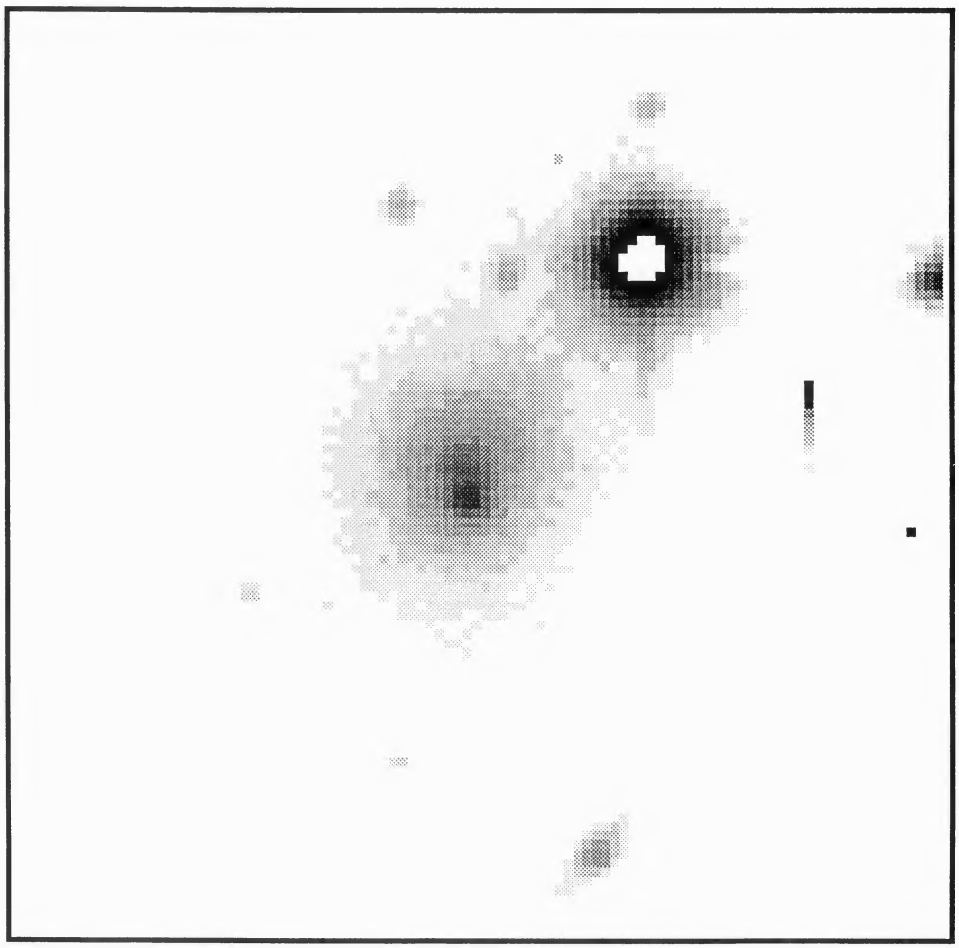

FIG. 5. Low contrast enhancement of the core of the cD galaxy in A2244. Shown is a 59 arcsec section of a 600 s Johnson V CCD frame from the Palomar 1.5 m telescope (north is at the top, east to the left). The imbedded companion is located 3 arcsec SSE from the center of the outer isophotes of the cD envelope (see discussion in text). The velocity of the companion relative to the cD velocity is 50 km s^{-1}. The overexposed object to the NE is a star.

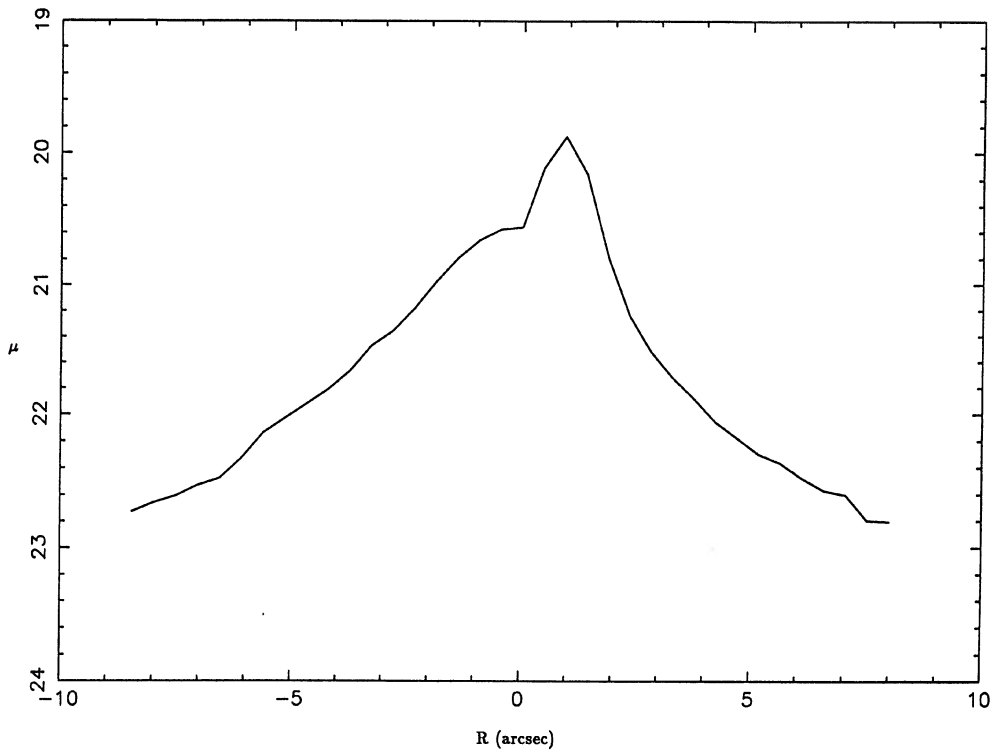

FIG. 6. Cross section of Fig. 5 in V mag arcsec^{-2} across the cD galaxy and companion. The inner surface brightness of the cD profile is 20.5 and for the companion is 19.8. The interpretation proposed is that the cD galaxy is undergoing a transition from a low-surface-brightness Ostriker–Hausman configuration to a higher core surface brightness due to increased central concentration from relaxation and surviving merger galaxies.

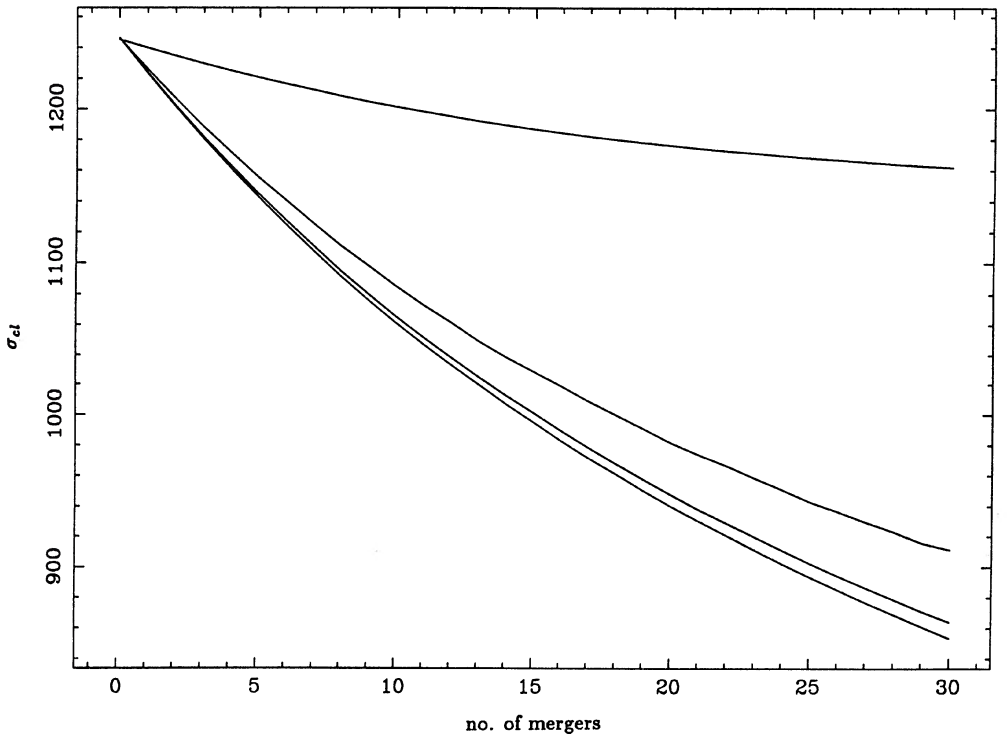

FIG. 7. Numerical simulation of adding low-velocity population members to A2244 as a function of resulting radial-velocity dispersion. Four populations with intrinsic dispersions of 1200, 500, 250, and 150 km s^{-1} are shown. In order to reduce the observed σ_{cl} in A2244 to the value of Coma (880 km s^{-1}) approximately 15–20 low-velocity objects must be removed from the cluster. This corresponds to between 8 and 10 L_* of luminosity that was consumed by the central cD galaxy.

but stays within the errors on σ_{cl}, indicates that the original data was overweighted with high-velocity members (i.e., not perfectly Gaussian in shape). However, only a true increase in the sample size can resolve this discrepancy. It is also notable that the number of missing members is very insensitive to the value of the bound population dispersion as long as it is less than $\frac{1}{2}\sigma_{cl}$. This is seen in Fig. 7 since the curves for 150 and 250 km s^{-1} are negligibly different from each other. To bring A2244's dispersion down to the Coma value of 880 km s^{-1} (Struble and Rood 1987b) requires 8–10 L_* of luminosity to have been cannibalized. This is similar to the total luminosity of the cD galaxy (10 L_*), although the common assumption is that the cD galaxy began with a seed object of 3–5 L_* (Schombert 1987).

c) Binaries

Before performing CCD imaging or spectroscopy, each binary was inspected on a PSS-II IIIa-J A grade plate. The purpose was to measure XY positions and determine position angles for the DBSP observations. However, during these measurements, it was noted that a number of the binaries were in fact galaxy/star pairs rather than galaxy/galaxy pairs. Overall, seven of the 18 binaries were found to be misidentified galaxy/star pairs. Examination of the old POSS plates showed that this was not due to errors in the original classification of Struble and Rood, but rather shows the significant advantage that the newer fine-grained emulsions of the PSS-II plates have over the old, coarse-grained 103a plates. Future studies of clusters will strongly benefit from T emulsion plates currently under development. Note also that the galactic latitude of A2244 is much lower than Coma (Table IV) and, thus, the higher number density of stars increases the probability of chance projections. To test the new classifications, two galaxy/star pairs were chosen at random and confirmed spectroscopically to be stellar (see below).

The distribution of binaries as a function of the radius is shown in Fig. 8 (only real galaxy/galaxy pairs were used). If the binaries were projected cluster/noncluster pairs, then one would expect that the higher cluster density in the core would produce a peak in the distribution. In fact, the binaries are fewer in the core with a majority between 250 kpc and 1 Mpc from the cluster center. This could be taken as additional evidence that the central cD galaxies in depopulating the core of the cluster.

Nine of the remaining 11 galaxy/galaxy pairs (plus five of the galaxy/star pairs) were imaged with the Palomar 1.5 m CCD system. Figure 9 is a montage of these frames chipped to 47 arcsec square fields. These frames were used to determine the separation between the pairs of which the mean separation was measured to be 7.6 ± 1.2 kpc. This is smaller than the mean separation of brightest cluster binaries (16 ± 9 kpc) as determined by Struble and Rood (1981), but probably reflects the small sizes of the galaxies plus the definition of contact envelopes in identifying the sample.

For spectroscopic study, the list of binaries was divided by type. As stated above, seven of the binaries where found to be galaxy/star pairs (4, 5, 8, 12, 13, 15, and 17). Two were confirmed by spectra (4 and 5). One of the galaxy/galaxy

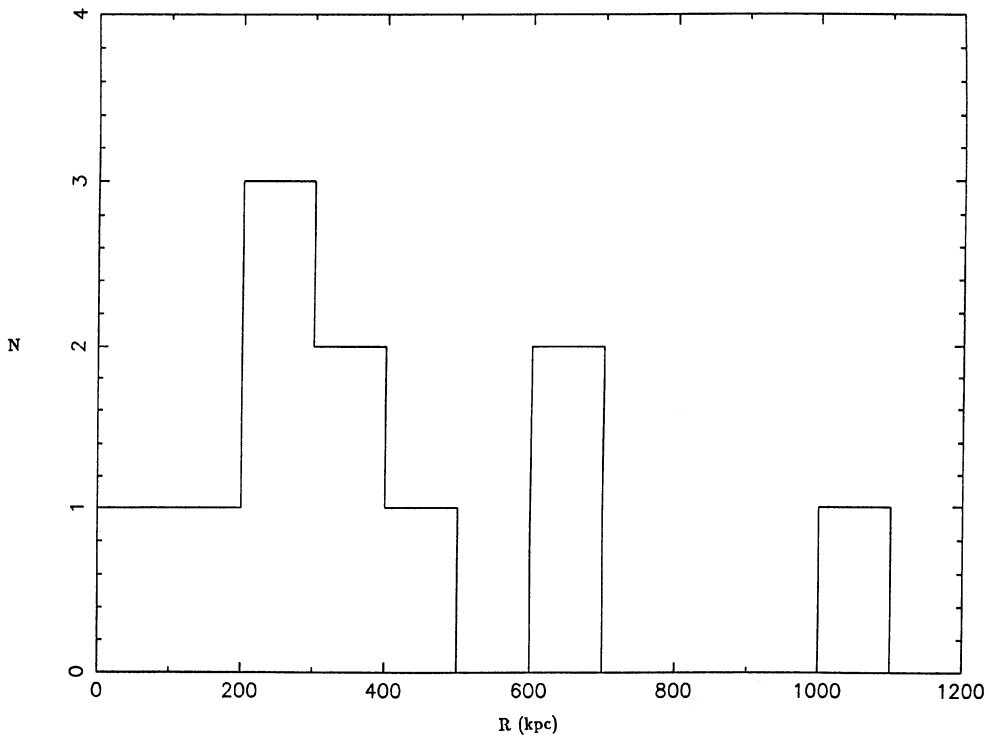

FIG. 8. Distribution of binaries with respect to projected distance from the cD galaxy. A majority of the binaries are not found in the high-density core region, as would be expected if they are pure projections, but rather at intermediate distances (mode at 250 kpc) from the center.

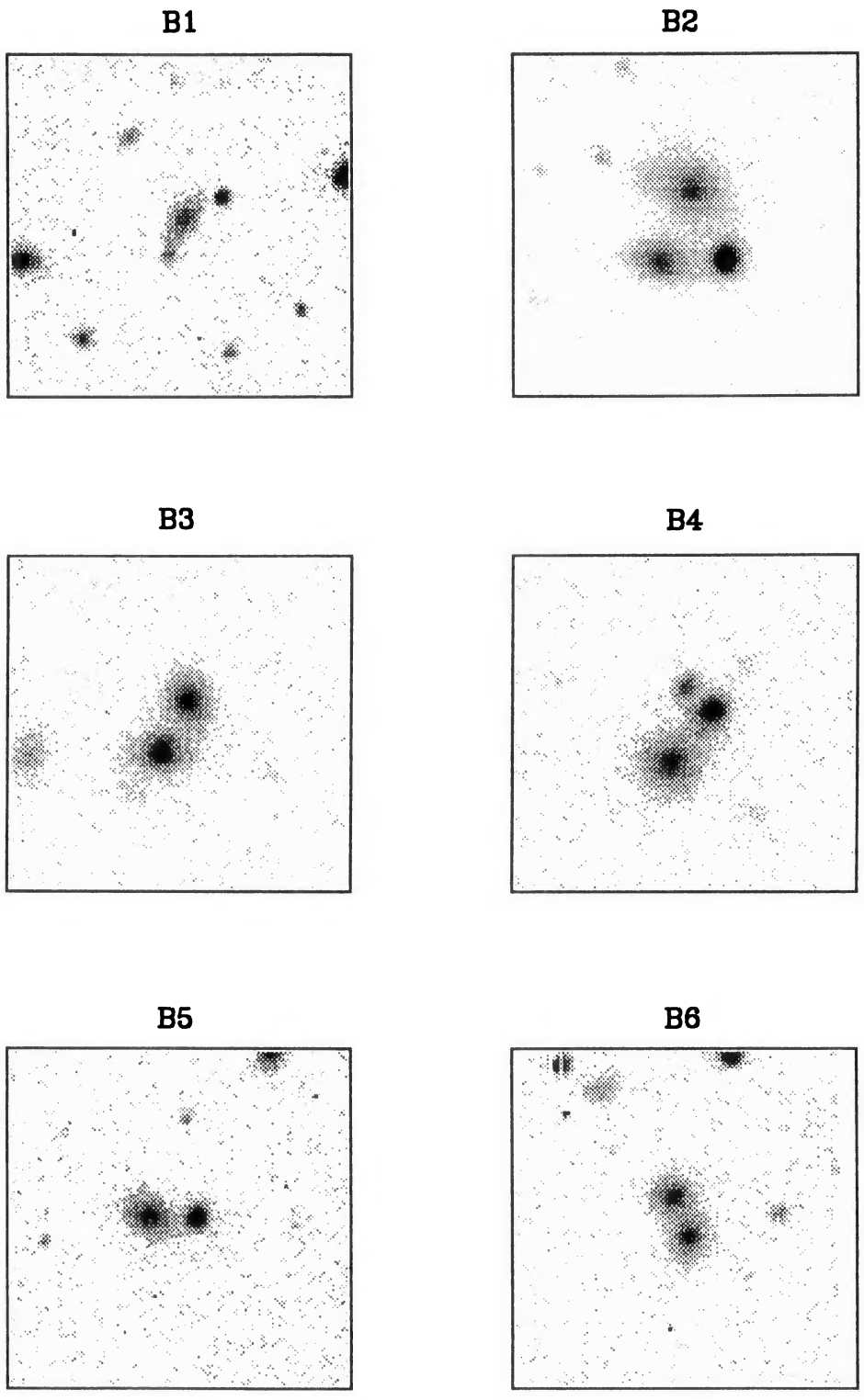

FIG. 9. CCD images for 14 of the 18 binary pairs in A2244. Each frame is 47 arcsec clipped from 300 s Johnson *V* exposures.

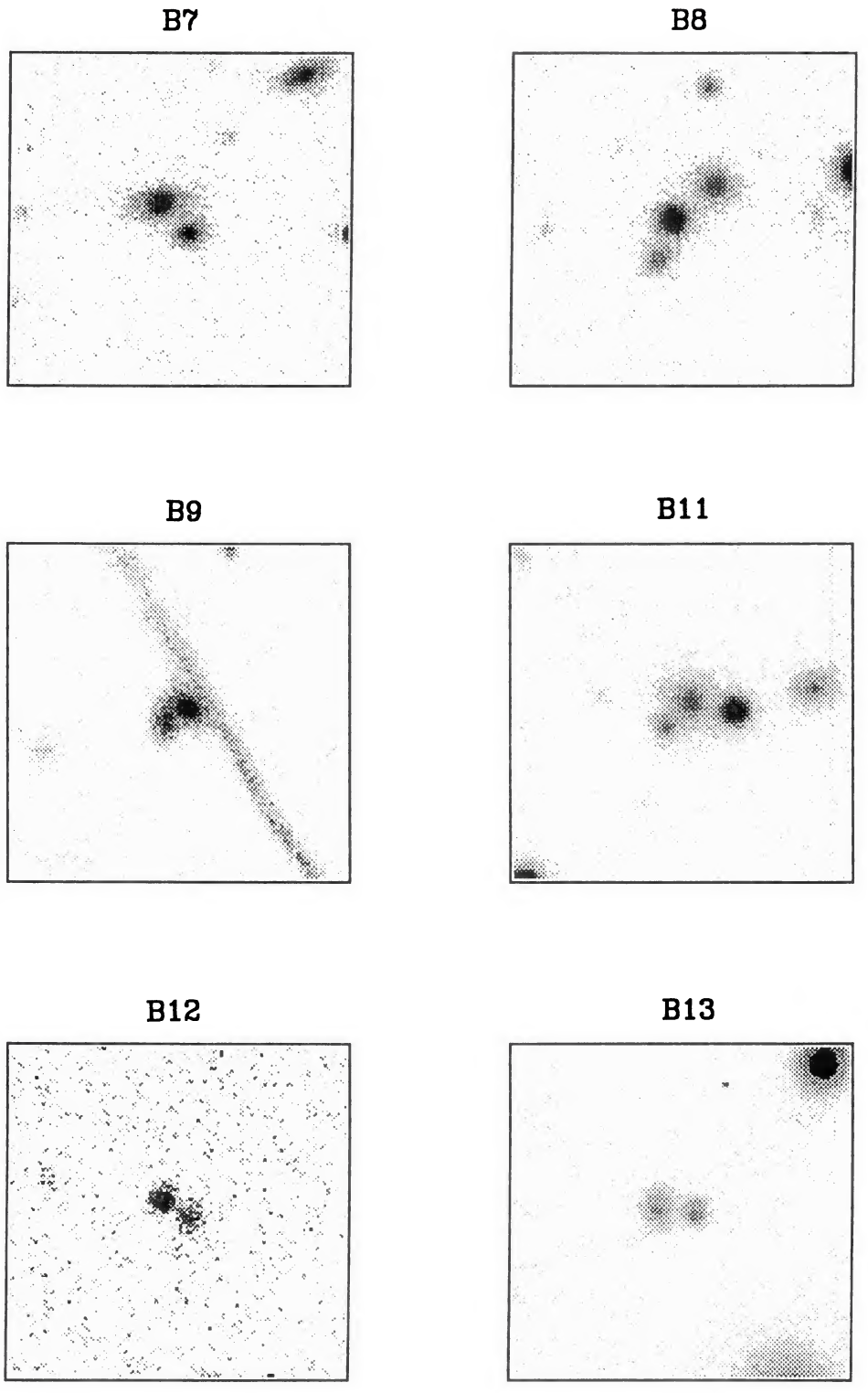

FIG. 9. (continued)

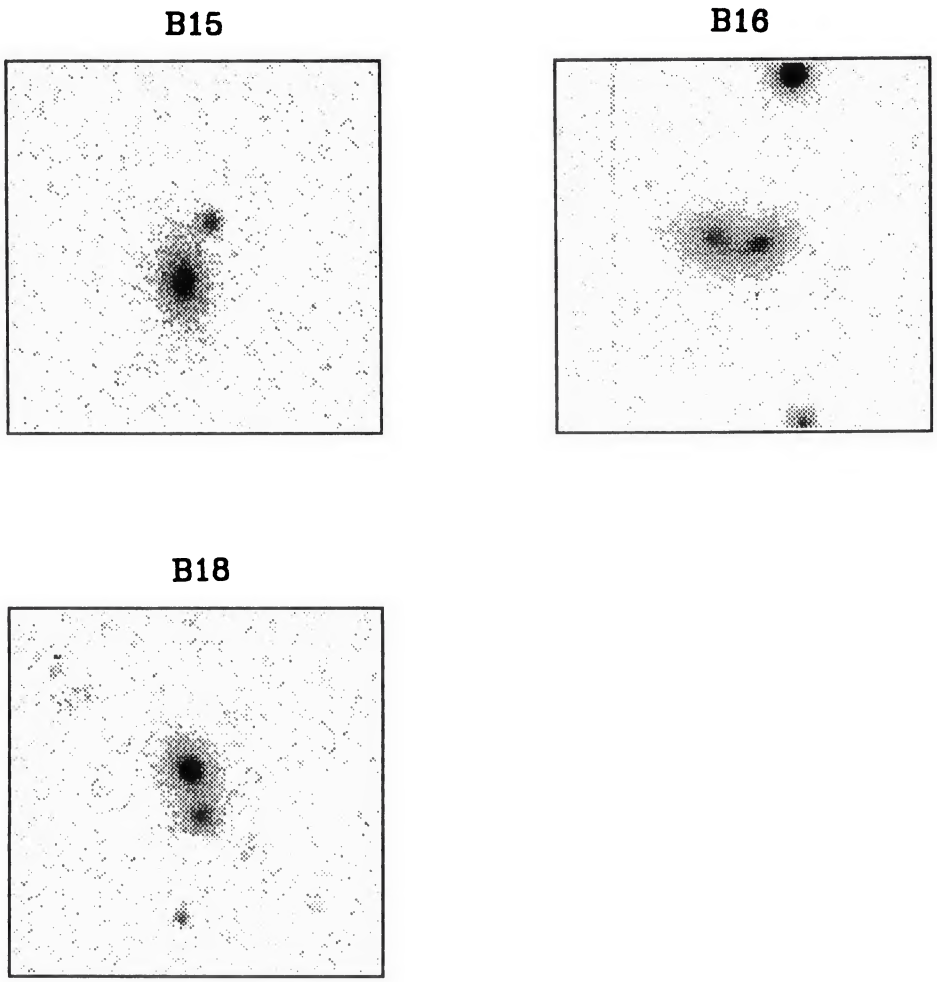

FIG. 9. (continued)

pairs was too faint (binary 1) and removed from the sample. Two more were not imaged and removed from the sample as well. The remaining eight binaries were measured (binaries 2, 3, 6, 7, 9, 11, 16, and 18) and are listed in Table II. The resulting line-of-sight velocity differences were (in order) 1866, 343, 2548, 1043, 16700, 65900, 200, and 2940 km s^{-1}. Clearly, with the exception of binary 16 (see Sec. III*d*), all the binaries have velocity differences in excess of the typical internal velocity of a galaxy (200–300 km s^{-1}) and, therefore, are most likely *not* bound pairs. Binary 3 can be included if the criteria of $\Delta v < 500$ km s^{-1} from Tonry (1985) is used. Two binaries (9 and 11) were projections of a cluster member with a background object. The rest are projections of cluster members.

Interestingly, all the binaries in this sample have the criteria of "common" envelope used by Struble and Rood (1981). Although the number of pixels in the CCD frames obtained in this study were too small to perform a detailed examination of distorted isophotes, all of the objects selected by Struble and Rood were enclosed by a common 25 V mag $arcsec^{-2}$ isophote. Hence, the above large velocities differences, which show that all but one or possibly two, objects are nonbound projected pairs, is quite surprising. The chance projection of two galaxies onto each others isophotes is usually a rare event and will be discussed further (see Sec. III*e*). A2244 should serve as a lesson to studies that attempt to interpret the occurrence of physical interaction based solely on projected association rather than differences in velocity space.

d) Binary 16

The only strongly bound pair in the binary sample is object 16. The velocity difference was determined to a high degree of accuracy from Hα emission. The top panel in Fig. 10 shows a reproduction of binary 16 from Fig. 9, the bottom panel is an extracted section of the two-dimensional spectra for the region surrounding Hα. The slit had been placed east–west directly across the nucleus of each galaxy. The pair is clearly interacting since the Hα emission can be traced spatially and dynamically through the envelopes of each component. It is also apparent in the same figure that the eastern component has discernable rotation.

The algorithm discussed in Sec. II*c* was used to produce velocity for each column of the CCD frame. Two such columns are shown in Fig. 11, high and low signal examples. The Hα, N [II], and S [II] features are marked plus the calculated best fits assuming Gaussian line profiles, fixed line centers, and widths. The residuals after continuum fit are also shown. The power of this technique lies in the fact that, for medium-to-high signal, the formal errors are less than 10 km s^{-1} ($\frac{1}{30}$ of a pixel).

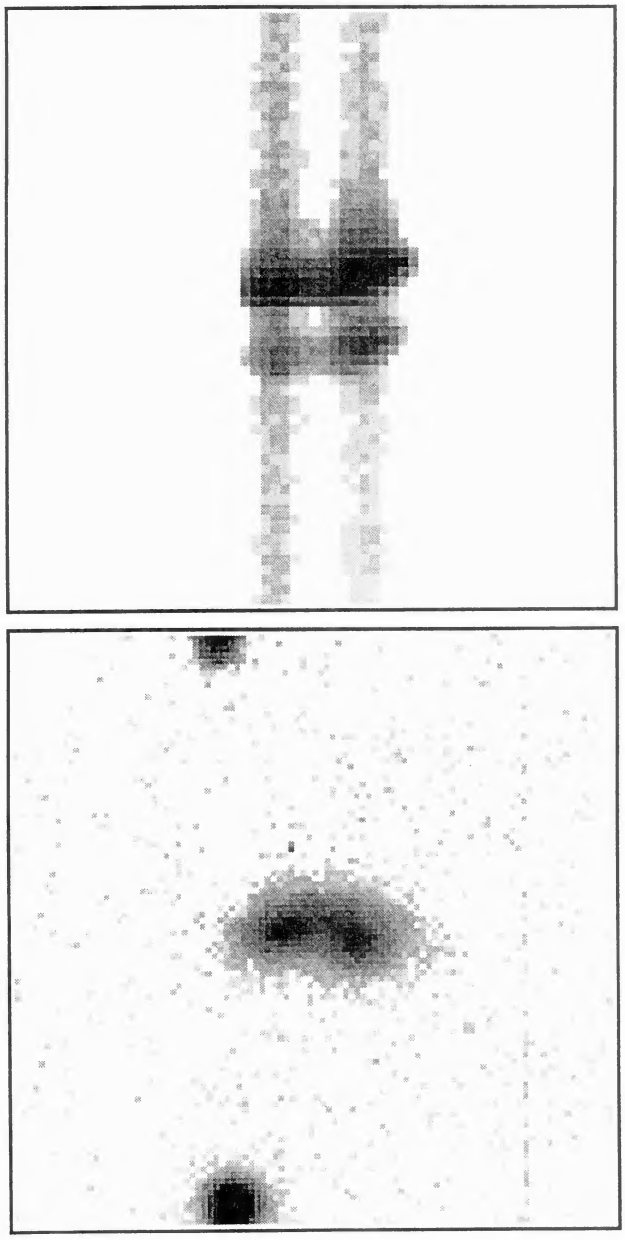

FIG. 10. Image of binary 16 from Fig. 8 plus a closeup of the 2D spectra center on Hα (spatial scales the same, red at the top). The Hα, N[II], and S[II] features are marked. Discernable rotation is visible in the easternmost galaxy. Also note that emission is continuous between the objects indicating a strong interaction.

The resulting spatial-velocity diagram is shown in Fig. 12. The bottom half of this figure shows the raw counts in the Hα feature as a function of radius. The spatial scale is plotted in arcsec with a conversion factor of 1.23 kpc per arcsec. A rotation curve for the eastern galaxy is clearly evident with a V_{max} around 160 km s^{-1}. The western component shows no obvious rotation, but has a continuous connection in velocity with its companion. The rotation curve for the eastern component is slightly unusual. Comparison with the rotation curves for spirals of the same brightness ($M_V = -19.5$) of Rubin *et al.* (1978) indicates that it has the correct V_{max} for its luminosity, but that the form of the rotation curve differs from the norm in the sense that it rises slower than normal spirals with a shallow solid-body portion. However, this is probably due to the fact that the slit did not exactly lie along the major axis, but rather is slanted 30°–40° from the major axis. Thus, some of the solid-body halo is contributing to the rotation measurement.

The $\mathcal{M}/L$ for the system is 10 ± 2 using the method of Schweizer (1987). The Hα emission crosses from east to west in a smooth fashion with no discontinuities. This implies either a strong, induced star formation event or both objects were star forming before the interaction and have mixed their envelopes. Current theory supports induced star formation and future projects to search for bound pairs may wish to consider Hα imaging as a prelude to spectroscopy for sample selection.

e) N-body Simulations

It is possible to make some estimates of just how frequently one would expect to see "binary" galaxies in the projected galaxy distribution of a rich cluster. Struble and Rood (1981) calculated the expected number of binaries using simple Poisson statistics and an assumed uniform density cluster. However, because the number of close pairs that are seen in projection depends sensitively on the actual cluster density profile, such calculations are not entirely appropriate. As a comparison to a more realistic "control" sample, we have instead calculated the expected number of projected binaries and their line-of-sight velocities from *N*-body simulations of clusters. Simulations of four rich clusters were taken from West, Dekel, and Oemler (1987). These simulations were each viewed from 100 different random orientations, and the distribution of pair separations and their relative velocities then calculated.

Results from these simulations are summarized in Figs. 13 and 14. The distribution of the projected pair separations d varies with the region of the cluster sampled in accordance with what one might expect from the cluster density profile. The top panel in Fig. 13 shows this distribution for three regions of a cluster; those pairs located 0–0.5 Mpc from the cluster center, 0.5–1 Mpc, and 1–3 Mpc. In general, pairs with small d's are found near the center of clusters, as would be expected since this is the region where the galaxy density is highest. If a binary is defined as any pair with $d < 20$ kpc, then 8.7% of the cluster members would have been identified as binaries (5.4%, 1.2%, and 2.1% for the above regions of the cluster). Scaled to the richness of A2244, the simulations predict 13 to 14 binaries to be cataloged from simple separation criteria, similar to the number found by Strubel and Rood. In the bottom panel of Fig. 13, those galaxies with projected separations of $d < 20$ kpc have been sorted out and their true separations D are plotted. From this subsample, 47% have true separations less than 20 kpc; or, in other words, 4.1% of all cluster members are, at any one time, within 20 kpc of a neighbor. This effect is, of course, more prominent in cluster cores.

This population of galaxies with $d < 20$ kpc can also be inspected for its kinematic properties. This is shown in Fig. 14, the distribution of line-of-sight velocity differences between pairs Δv_{LOS}, and the distribution of true velocity differences, Δv_{true}. The line-of-sight velocity distribution predicts that 18% of the projected binaries would have measured velocities less than 400 km s^{-1} although less than 0.1% of the sample have true velocities less than 400 km s^{-1}. Scaled to A2244 values, this implies that at most 2 or 3 binaries would have low-velocity differences, exactly as is seen in

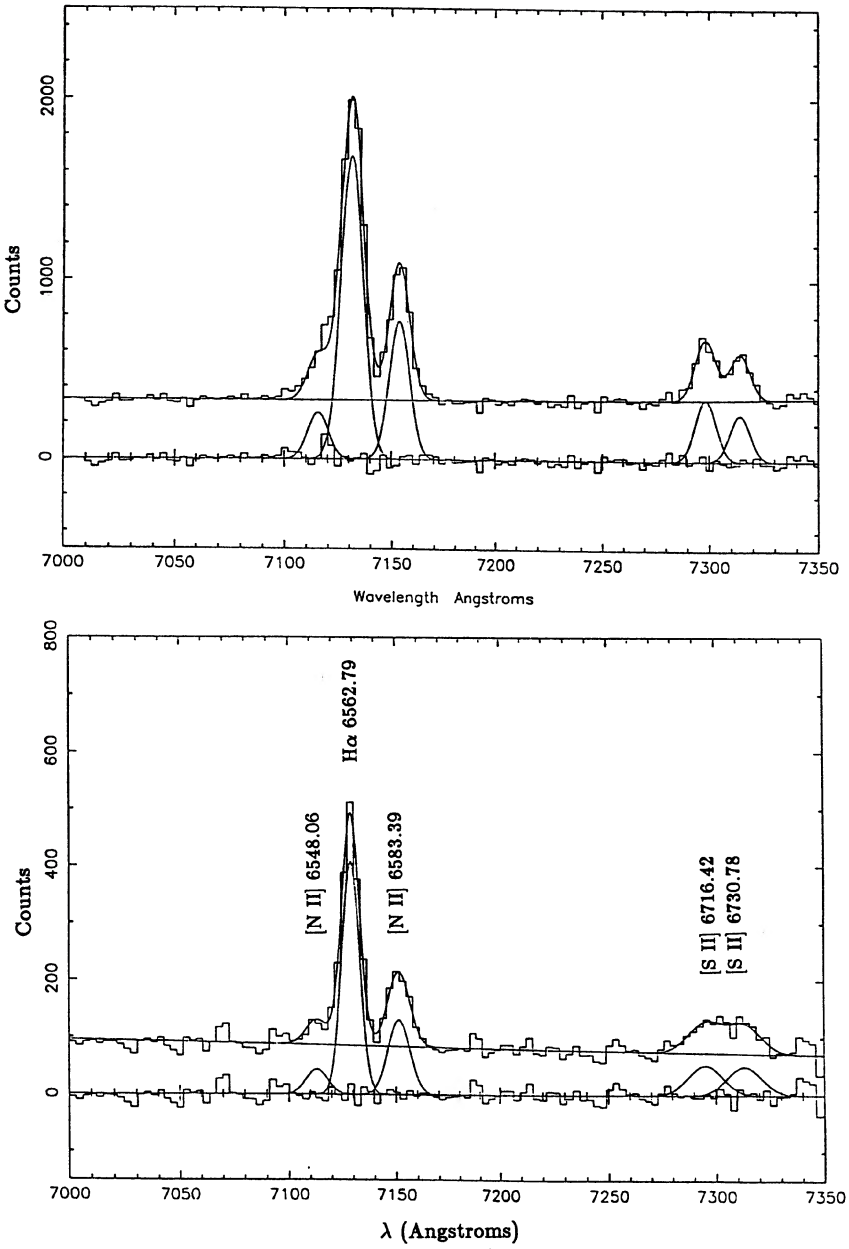

FIG. 11. High and low signal-to-noise examples from extracted columns of the spectra in Fig. 9. Fits by the algorithm discussed in the text plus residuals are shown.

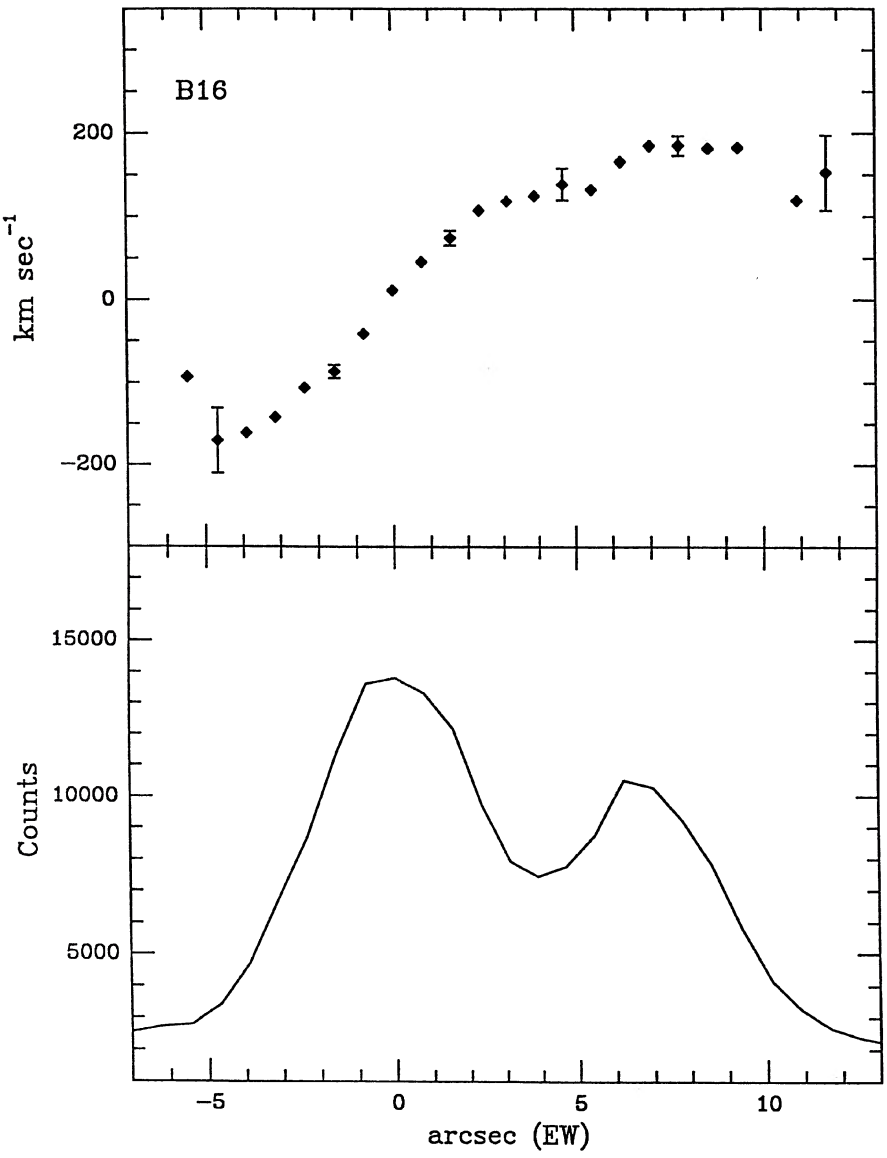

FIG. 12. Resulting spatial-velocity diagram (top) and raw Hα counts (bottom) for binary 16. The rotation for the easternmost galaxy is obvious with a V_{max} of 180 km s^{-1}, similar to values for $M_V = -19.5$ objects from Rubin *et al.* (1978). A velocity difference of 200 km s^{-1} is also visible.

Table II. Therefore, the separation and velocity information presented above is consistent with the conclusion that none of the binaries are bound configurations. Only the suggestive interactive Hα features in B16 supports a real binary in that one case.

IV. CONCLUSIONS

This paper presented a dynamical study of the cluster of galaxies A2244, a system supposedly rich in binary pairs from the list of Struble and Rood (1981). In addition, we have also examined the central cD galaxy of these clusters and how its features reveal clues to the origin and evolution of first-ranked galaxies and the evolution of the dynamics of the core of the cluster. The results can be summarized as follows.

(1) Although A2244 is only 63% of the richness of Coma, they are similar in their coarse morphological properties. Both Coma and A2244 are most likely clusters of an advanced postcollapse nature. They have similar Rood–Sastry types (*B* and cD) and have identical Bautz–Morgan types (Type II). Both have evidence of weak mass segregation in their cores, and both have a centrally located cD galaxy of identical size and magnitude.

(2) However, Coma and A2244 differ in a fashion that may be related to the formation of the cD galaxy. A2244 is deficient in the projected density of galaxies in its core relative to Coma. And, since A2244 is only 28% of the core luminosity of Coma (versus being 84% of the global richness or 42% of the core number density), there is evidence that the deficiency is in bright galaxies. A2244 has a radial-velocity dispersion of 1240 km s^{-1} versus Coma's value of 880 km s^{-1}. Numerical simulations suggest that if a bound population of low-velocity objects ($\Delta v < 300$ km s^{-1}) once existed of the type found in A2589 (Bothun and Schombert 1988), then 8–10 L_* of luminosity was available to be consumed for the formation of the cD galaxy.

(3) The cD galaxy has an unusual shape with an apparent

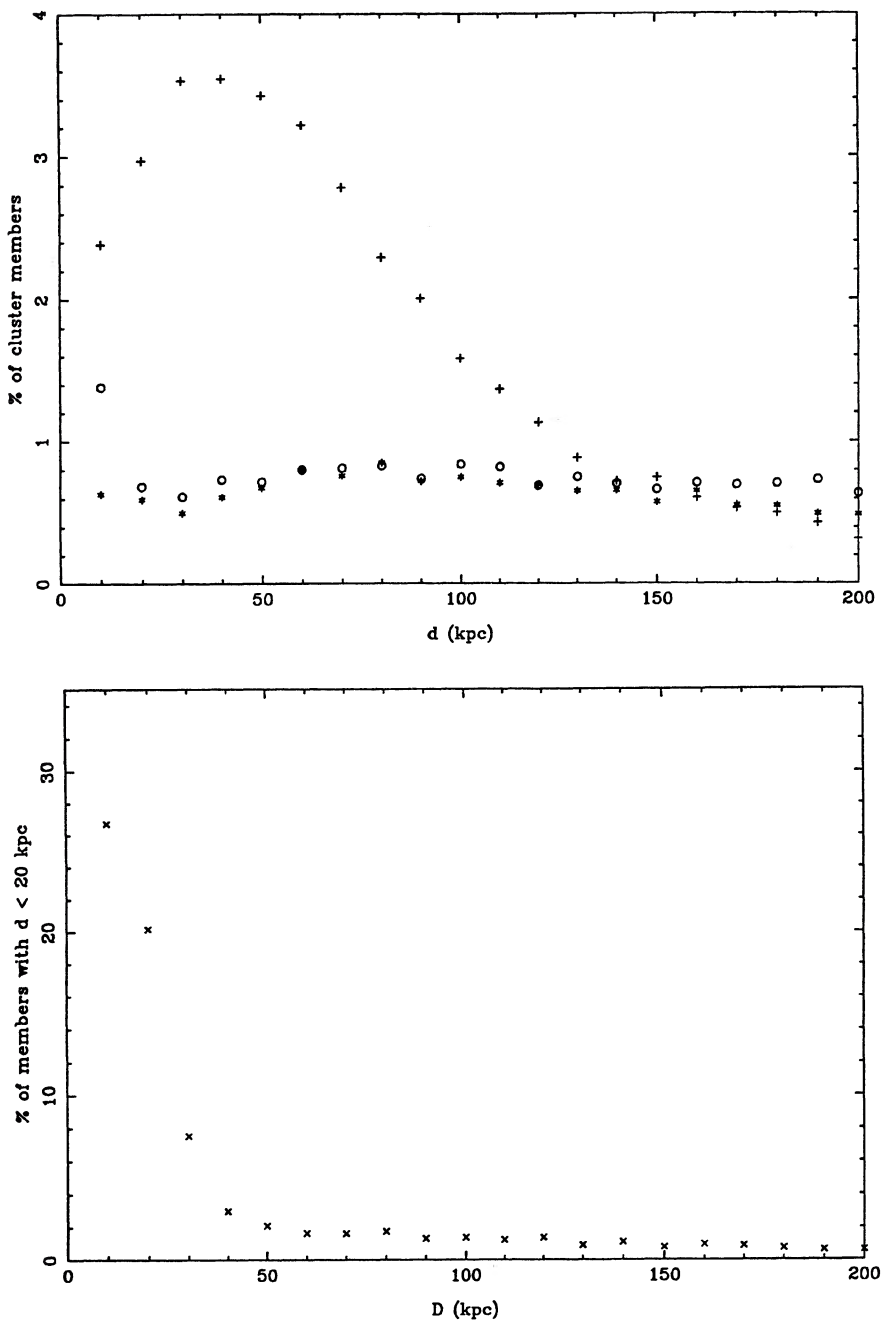

FIG. 13. Top panels show the run of projected separations for three regions of a cluster (+ = 0–0.5 Mpc, * = 0.5–1.0 Mpc, and O = 1.0–3.0 Mpc) as a function of the percentage of total cluster members. This plot is based on the *N*-body simulations from West *et al.* (1987). The bottom panel shows the true separations for all objects in the simulations with projected separations less than 20 kpc. Overall, 8.7% of cluster members should appear as projected binaries with 47% of the projected pairs actually being close in real space.

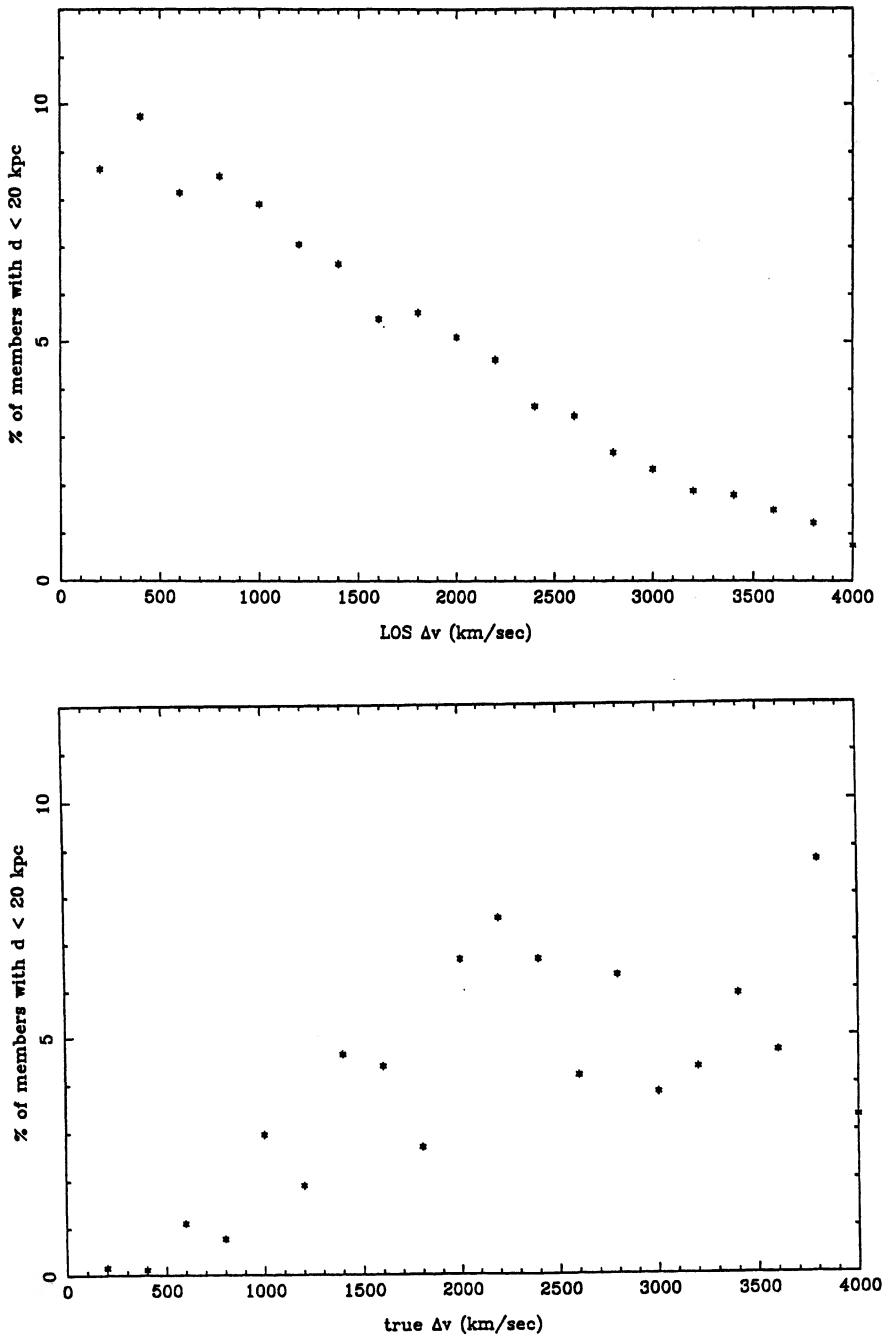

FIG. 14. Top panel shows the line-of-sight velocity differences for all objects in the simulations with projected separations less than 20 kpc. Only the bottom panel shows the true velocity difference for the same sample.

off-axis core. This core is most likely an infalling companion galaxy with a Δv of 50 km s^{-1}, presumably close to a final merger stage. The interpretation of the cD galaxy structure is that the system is undergoing a transition from a depressed central surface-brightness profile to one suggested by White (1982) and the simulations of Duncan, Farouki, and Shapiro (1983) of high central surface-brightness with a shallow profile slope.

(4) Of the binaries studied, 39% were misclassified galaxy/star pairs, 53% were unbound projected pairs (38% cluster projections, 15% background projections), and only 8% (one object) were true bound systems. Therefore, the conflict between normal cluster formation scenarios that inhibit binary formation and the existence of a binary-rich cD cluster does not exist. Binaries are still rare in evolved clusters.

(5) The one bound binary (binary 16) is a clear example of strong star-formation activity that is associated with an interaction. A continuous connection between the components, spatial and in velocity, confirms their bound nature.

(6) Comparison to *N*-body simulations indicates that the observed numbers of projected binaries and the distribution of line-of-sight velocities is exactly as would be expected from projection effects in a typical rich cluster.

The authors wish to thank Juan Carrasco for superb handling of the Palomar 5 m telescope. We also thank G. Helou for sharing some of his telescope time.

REFERENCES

Abell, G. O. (1958). Astrophys. J. Suppl. **3**, 211.
Beers, T. C., and Tonry, J. L. (1986). Astrophys. J. **274**, 491.
Bothun, G. D., and Schombert, J. M. (1988). Astrophys. J. **335**, 617.
Cawson, M. (1983). Ph.D. thesis, University of Cambridge.
Danese, L., De Zotti, G., and di Tullio, G. (1980). Astron. Astrophys. **82**, 322.
Duncan, M. J., Farouki, R. T., and Shapiro, S. L. (1983). Astrophys. J. **271**, 22.
Fitchett, M. J., and Webster, R. L. (1987). Astrophys. J. **317**, 653.
Godwin, J. G., and Peach, J. V. (1977). Mon. Not. R. Astron. Soc. **181**, 323.
Heggie, D. (1975). In *Dynamics of Stellar Systems*, Proceedings of the IAU Symposium No. 69, edited by A. Hayli (Reidel, Dordrecht), p. 95.
Hickson, P. (1977). Astrophys. J. **217**, 16.
Landolt, A. (1985). Astron. J. **88**, 439.
Lecar, M. (1975). In *Dynamics of Stellar Systems*, Proceedings of the IAU Symposium No. 69, edited by A. Hayli (Reidel, Dordrecht), p. 161.
Leir, A. A., and van den Bergh, S. (1977). Astrophys. J. Suppl. **34**, 381.
Massey, P., Strobel, K., Barnes, J. V., and Anderson, E. (1988). Astrophys. J. **328**, 315.
Oemler, A. (1976). Astrophys. J. **209**, 693.
Oke, J. B., and Gunn, J. E. (1982). Publ. Astron. Soc. Pac. **94**, 586.
Ostriker, J. P., and Hausman, M. A. (1977). Astrophys. J. Lett. **217**, L113.
Porter, A. (1988). Ph.D. thesis, California Institute of Technology.
Postman, M., Geller, M. J., and Huchra, J. P. (1989). Preprint.
Rubin, V. C., Ford, W. K., and Thonnard, N. (1978). Astrophys. J. Lett. **225**, L107.
Schombert, J. M. (1986). Astrophys. J. Suppl. **60**, 603.
Schombert, J. M. (1987). Astrophys. J. Suppl. **64**, 643.
Schombert, J. M. (1988). Astrophys. J. **328**, 475.
Schweizer, L. Y. (1987). Astrophys. J. Suppl. **64**, 427.
Struble, M. F. (1979). Astron. J. **84**, 27.
Struble, M. F., and Rood, H. L. (1981). Astrophys. J. **251**, 471.
Struble, M. F., and Rood, H. L. (1987a). Astrophys. J. Suppl. **63**, 543.
Struble, M. F., and Rood, H. L. (1987b). Astrophys. J. Suppl. **63**, 555.
Tonry, J. L. (1985). Astron. J. **90**, 2431.
Tonry, J. L., and Davis, M. (1979). Astron. J. **84**, 1511.
West, M. J., Dekel, A., and Oemler, A. (1987). Astrophys. J. **316**, 1.
White, S. D. M. (1979). Mon. Not. R. Astron. Soc. **189**, 831.
White, S. D. M. (1982). In *Saas–Fee Lectures*, edited by L. Martinet and M. Mayor (Geneva Observatory, Geneva), p. 291.
White, S. D. M., Huchra, J., Latham, D., and Davis, M. (1983). Mon. Not. R. Astron. Soc. **203**, 701.
Zabludoff, A. I., Huchra, J. P., and Geller, M. J. (1989). Preprint.